Investigation of microstructure and mechanical properties of multi-pass friction stir processing on precipitation hardened aluminum alloy

Vipin Sharma[1*], Yogesh Dewang[2], Mohit Sharma[3], Yashpal Gupta[4]

[1] Associate Professor, Department of Mechanical Engineering, Medi-Caps University, Indore-453331, India

[2] Associate Professor , Department of Mechanical Engineering, Lakshmi Narain College of Technology, Bhopal

[3] Assistant Professor, Department of Mechanical Engineering, Medi-Caps University, Indore-453331, India

[3] Assistant professor, Department of Mechanical Engineering, Panipat Institute of Engineering & Technology, Panipat, India

Abstract

In the present study, multi-pass friction stir processing of aluminum AA2014-T651 alloy is performed with one and four passes. The multi-pass processing is performed at a tool rotational speed of 1000 rpm with a traverse speed of 63 mm/min. Microstructural characterization of friction stir processed specimens indicated a significant grain refinement with equiaxed grains in the four pass specimen. Microhardness and tensile strength of the multi-pass specimen decreases with the increase in number of passes. Fracture toughness of the multipass specimen exhibited a decrease in the fracture toughness on increasing the number of passes. Hardening precipitates in the base alloy govern the mechanical properties and contribution of the grain refinement to strength, hardness and fracture toughness is limited. Thermal cycles experienced in the multi-pass friction stir processing affect the role of hardening precipitates.

Keywords:*friction, stir, processing, FSP, multipass, aluminum, Al-Cu*

****Author for Correspondence :*** V. Sharma, Medi-Caps University,
vipinsati@gmail.com, vipinsharma@medicaps.ac.in

INTRODUCTION

Friction stir processing (FSP) is a solid-state technique that alters the microstructure of materials applying frictional heat and stirring action of a tool **[1, 2]**. The FSP is a modified form of friction stir welding (FSW) which is originally developed by The Welding Institute in 1991 **[2, 3]**. Its procedure is simple consists of insertion of a rotating tool in the workpiece. Frictional heat is generated which softens the material and this material is stirred by the tool probe. In FSP, a cylindrical tool consists of concentric probe and shoulder which is placed into the material at as a certain rotating speed and in a particular direction. The temperature of the material is raised by generation of localized heat due to friction between the tool and the material. In FSP, the achieved high temperature is responsible for severe plastic deformation which significantly refines grain by dynamic recrystallization mechanism **[4, 5]**.

The two main purpose of the FSP tool are heating and deformation of processed material. The increase in temperature due to heat generation, softens the material and this softened material is also stirred by rotating tool. In friction stir processing the material softens but remains in the solid state. The softened material helps to fill produced cavity during FSP at the rear of the tool with the traverse movement of tool in forward direction **[6, 7]**. The material is subjected to intense heat exposure and plastic deformation, which greatly refines the microstructure **[7, 8]**. FSP is also a combination of deformation, stirring, extrusion, forging and consolidation processes. The probe stirs the softened material while tool axial force provides forging action. Processed zone can be considered analogous to an extrusion chamber surrounded by cold material (unprocessed material) and tool. The softened material is stirred and extruded as the tool moves forward, and this extruded material forms a processed zone **[7]**. There are various FSP parameters which affect the resultant microstructure and properties of the material. In FSP, rotational speed, traverse speed, tool geometry, and number of passes are primary parameters. The number of passes or multi-pass is an important parameter in FSP of materials and fabricating surface composites **[9, 10]**.

Multi-pass FSP exhibits the enhanced mechanical properties due to better grain refinement and homogeneous distribution of second phases **[11-13]**. The FSP also reduces microstructural inhomogeneity and clustering of the reinforcement particles in the metal matrix composites **[12, 13]**. **Faraji et al. [11]** pointed out that homogenized and ultra fine grain microstructure is effectively produced by the increasing the number of pass in FSP. In multi-pass FSP optimum number of FSP pass provide the improved properties and further, increasing the FSP pass may deteriorate the properties. Commonly, four pass FSP is considered as the optimum FSP pass for multi-pass FSP. In study of the multi-pass FSP of WE43 magnesium alloy, **Eivani et al. [14]** demonstrated that four pass FSP is sufficient for grain size refinement. They applied six pass of FSP and found that after four pass the grain size reduction is limited. The average grain size dropped from 12.4 to 1.4 μm after four FSP runs and even further increase to 6 passes showed no significant changes. However, throughout the fourth and sixth FSP passes, second-phase particle fragmentation and redistribution continued. **Cui et al. [15]** showed that two pass FSP had better strength as compared to single pass in multi-pass FSP of A356 alloy. They also found that on further increasing passes beyond two passes the microstructural refinement and increase in strength was not significant.

In multi-pass FSP, percentage of overlapping is also investigated and various overlapping percentages such as 100 %, 50%, 75% etc., were used **[16, 17]**. **Venkateswarlu et al. [16]** reported that 100% overlapping multi-pass showed better mechanical properties and formability as compared to other ratios in friction stir processed AZ31B alloy due to better homogenization. According to **Gandra et al. [17]**, the 50% overlapping at the advancing side made a more uniform thickness while overlapping at the retreating side formed smoother surfaces. However, the advancing side had shown the better mechanical property homogeneity as compared to the retreating side. As per the study of Jana et al. [18], stability of microstructure in stir zone of F357 alloy at an elevated temperature is controlled by multi-pass FSP. They reported that abnormal grain growth (AGG) in the stir zone (SZ) produced by single pass FSP cross-sections when it was exposed to elevated temperatures, whereas it was not observed in produced stir zone by multi-pass FSP after an exposure to an elevated temperature. Hu et al. [19]performed multi-pass FSP on Mg-Li alloy by probe-less FSP tool and found that FSPed alloy exhibited improved mechanical properties and corrosion resistance. The grain size was decreased from 38.26μm to 18.71 μm after multi-pass FSP. They attributed grain refinement and solid-solution strengthening for the improvement in mechanical properties. The elongation increased to 109.2% while the material's flexibility was substantially improved. To achieve uniform distribution of the reinforcement particles in surface composite fabrication the multi-pass FSP is used. **Mehdi et al. [20]** homogeneously dispersed ZrB_2 nanoparticles and fine grain structure was achieved by the multi-pass FSP of AA6082. They reported that ultimate tensile strength (UTS) was increased from 191 MPa of base alloy to 266 MPa. The four pass FSP is required to achieve the improved properties.

The multi-pass FSP can be a suitable strategy to achieve grain refinement and uniform distribution of second phases in metal matrix. In this study, microstructural and mechanical properties of the multi-pass FSP of precipitate hardened Al-Cu (AA2014-T651) alloy are investigated. The mechanical properties including hardness, tensile strength and fracture toughness of the friction stir processed (FSPed) specimens are correlated with one pass and four pass FSP.

2. EXPERIMENTAL

A6.30 mm plates of the chemical composition AA2014-T651 were employed in this investigation for both single-pass and multi-pass friction stir processing and a typical FSP is depicted in **Fig. 1**. In FSP, the applied tool is made of AH13 steel following specifications: 3 mm length for round bottom conical pin, 21 mm diameter for concave shoulder, a 5 mm and 3 mm top and bottom diameter respectively for conical pin and 55 HRC is used and a schematic of tool is provided in **Fig. 2**. The processing of the work-piece was conducted on a conventional vertical milling machine (Hindustan machine tools, India) at a constant 1000 rpm and 63 mm/min of tool rotational and traverse speed, respectively. When using several passes of FSP, the preceding FSPed zone is completely (100%) overlapped by the four FSP passes.

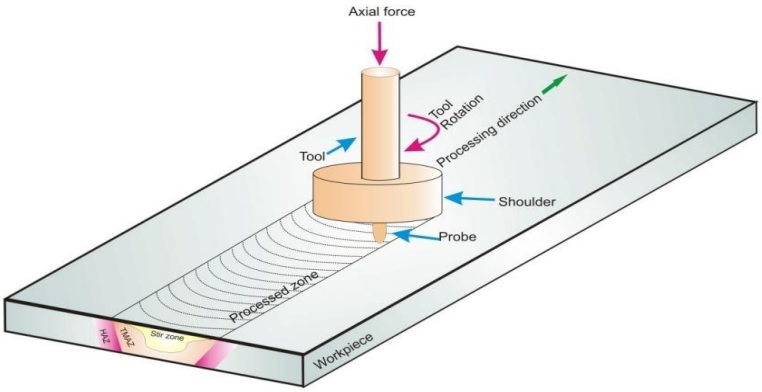

Fig.1: Schematic of FSP for processing work-piece plate.

The microstructural investigation of perpendicularly cut samples to the processed direction was carried out of using an optical microscope (LEICA DMI5000 M) and a scanning electron microscope (SEM, Zeiss EVO 18). The specimens were ground and polishing upto 1 micron following a standard procedure and further etched by freshly prepared modified poulton's reagent. The mean linear intercept method was applied to calculate the average grain size as per ASTM standard. Vickers microhardness tests were performed utilizing an Omnitech India MVH-II Vickers microhardness tester with an applied load of 200 gf and a dwell duration of 15 seconds. H25 K-S; Hounsfield Test Equipment, Ltd., Surrey,UK, universal testing machine was employed for tensile tests. The dimensions of the tensile test specimen are shown in **Fig. 3 (a)**. Fracture toughness was evaluated by fatigue test of compact tension test specimens (CT) with notch were prepared of base alloy and friction stir processed (FSPed) specimens as shown in **Fig. 3 (b)** by Universal testing machine (Instron 1342). In relation to the direction of plate rolling, specimens were machined in the same direction. All FSP specimens are machined from the crown side to remove flash, ensuring that the sides of the CT specimens are parallel to one another and that the final specimen thickness is 6 mm. In the center of the SZ, a spark technique is used to prepare a chevron-shaped notch. After around 25000 cycles of application, the fatigue pre-crack is produced by using a load ratio of R=0.1. 0.1 kN/s loading rate was maintained throughout the fracture toughness tests.

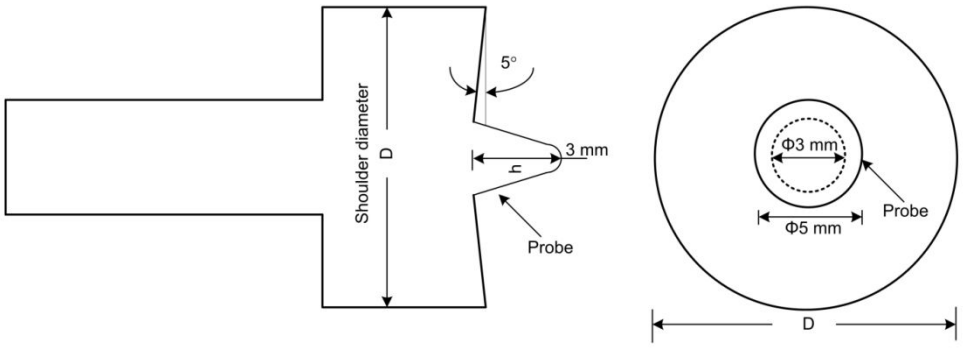

Fig. 2: Tool geometry dimensions used for friction stir processing.

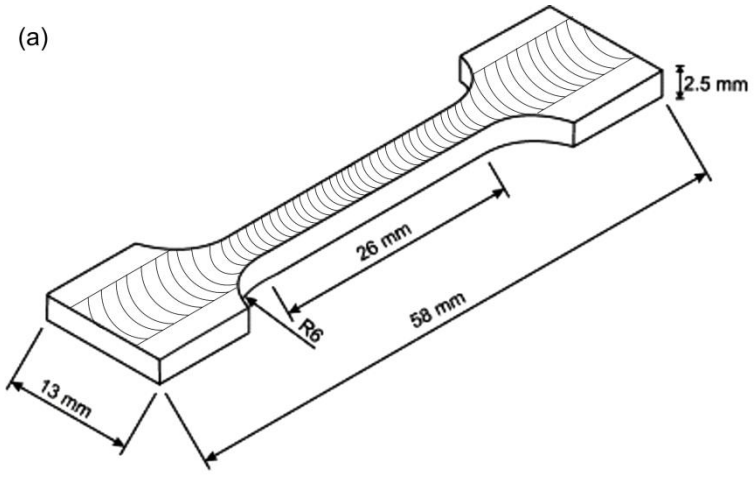

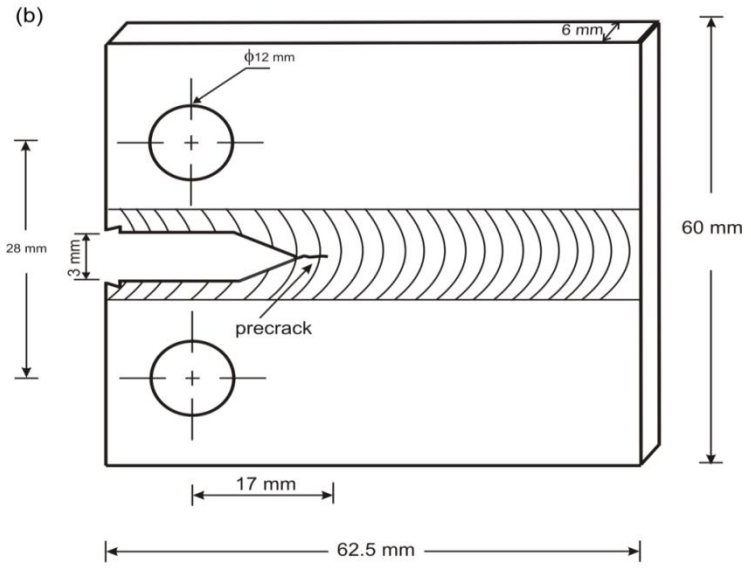

Fig. 3: Dimensions of the test specimens

(a) Tensile test specimen and (b) compact tension (CT) specimen.

3. RESULTS AND DISCUSSION:

3.1 Microstructure:

Macrographs of one pass and four passes of FSPed specimens exhibiting various microstructural zones are shown in **Fig. 4 (a, b)**. Shoulder affected zone (SAZ), thermo-mechanical affected zone (TMAZ), heat affected zone (HAZ), advancing side (AS) and retreating side (RS) are shown in macrographs. It is clearly evident from the macrographs that the SZ area of a four pass FSPed specimen is more than that of one pass FSPed specimen. A tilted oval shaped and distinct SZ is discernible in one pass FSPed specimen whereas semi-circular SZ is observed for four passes of FSPed specimen. The SAZ is also increased in four passes of FSPed specimen in comparison to one pass FSPed specimen. In four passes of FSP, repeated thermal cycles and plastic deformation resulted in increased SZ area. The material flow in SZ is governed by shoulder driven and probe driven flow. Repetitive thermal cycles with intense plastic deformation may results in merger of SAZ and SZ in four pass FSP.

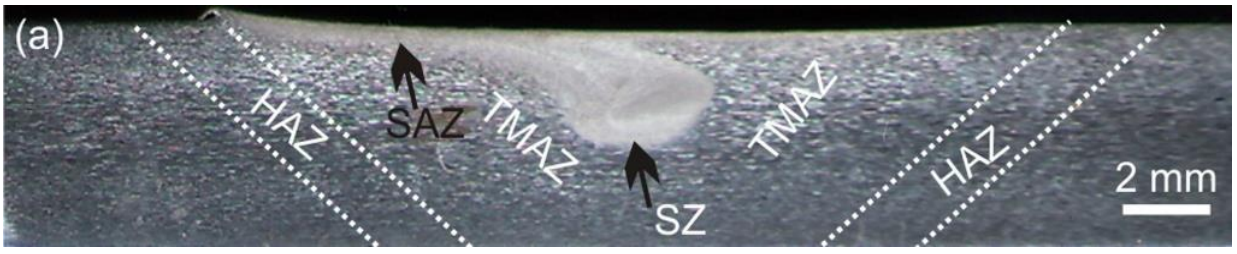

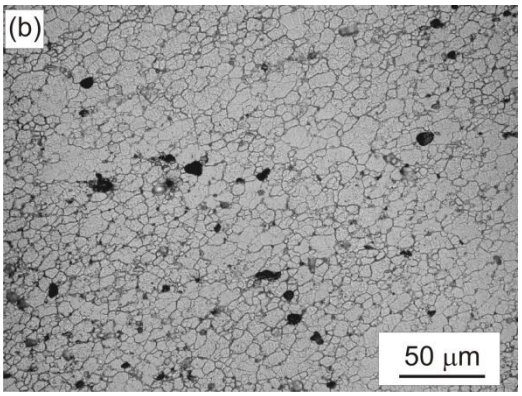

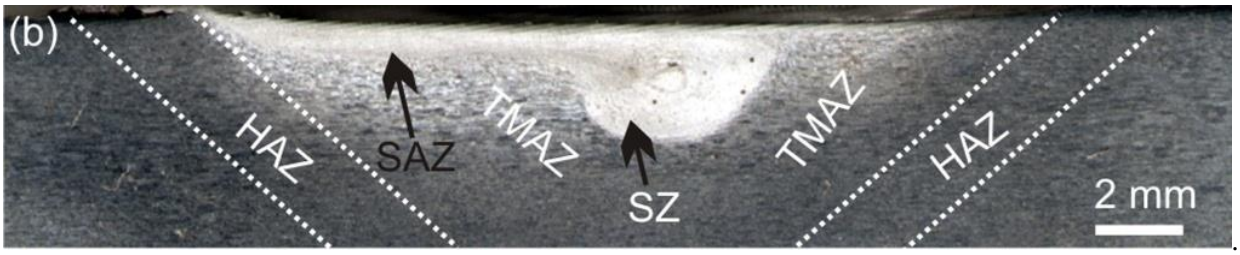

Fig. 4: Macrograph of FSPed specimens exhibiting various microstructural zones (a) one pass and (b) four passes.

Optical micrographs of base alloy, SZ after one pass and four passes of FSP are shown in **Fig. 5 (a-c)**. Micrograph of the base alloy AA2014 as shown in **Fig. 5 (a)** have an uneven grain size distribution with coarse precipitates. In base alloy the average grain size was found to be 125 μm due to the rolled sheet. Using EDS analysis, these precipitates were confirmed to be composed of Al-Cu, Al-Cu-Mg-Si and Al-Fe-Mn-Cu-Si. A representative image of EDS analysis of precipitates in base alloy is shown in **Fig. 6**. After one pass of FSP the grain size significantly reduces to ~12 μm but grain size distribution is not uniform in the SZ (**Fig. 5b**). Some of the precipitates dissolve and disperse when exposed to high temperatures and stirred, but there are still some small amounts of coarse precipitates. The formation of fine grains in SZ is ascribed to the dynamic recrystallization mechanism **[21-23]**. Micrograph of SZ after four passes of FSP as shown in **Fig. 5 (c)** exhibits a more uniform grain size distribution with the average grain size of ~7 μm. The grain size reduction after four passes of FSP is attributed to the repeated severe plastic deformation and dynamic recrystallization after each FSP pass. More grain boundary area is available after each FSP pass, resulting in increase of dislocations density as grain boundaries are the source of dislocations. It is also suggested that in aluminum alloys due to high stacking fault energy occurrence of dynamic recovery arranges dislocations into sub-grain boundary configuration **[23]**.

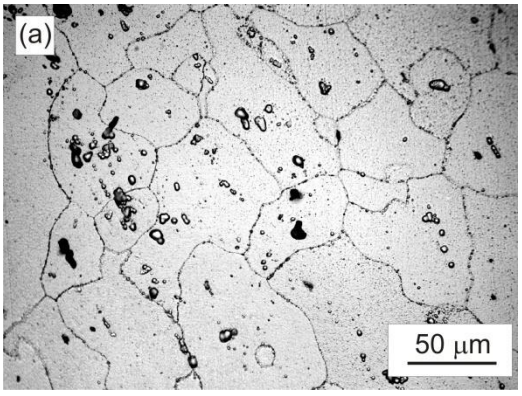

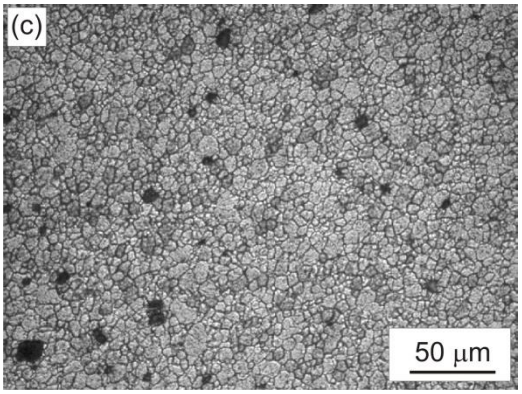

Fig. 5: Optical micrographs of base alloy and FSPed specimens (a) base alloy (b) one pass and (c) four passes.

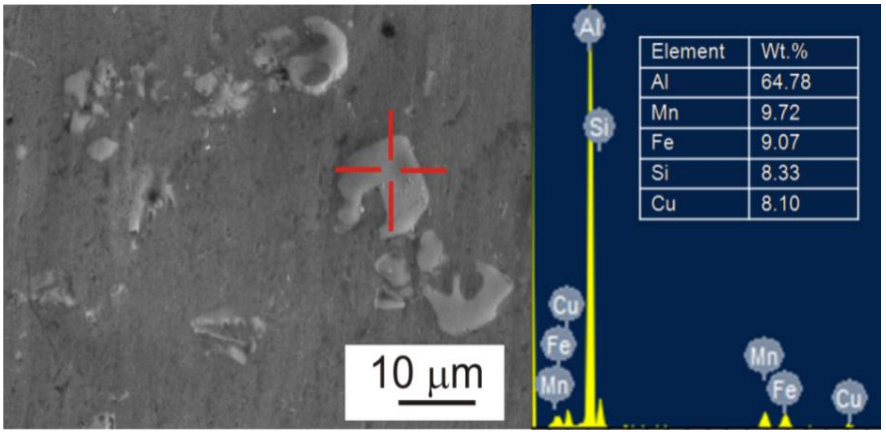

Fig. 6: SEM micrograph and corresponding EDS analysis of precipitate in base alloy**.**

3.2 Hardness:

Figure 7 shows the Microhardness of the base alloy and FSPed specimen. Four pass FSP specimen shows less hardness as compared to base alloy and one pass FSP specimen.The one pass FSP specimen exhibits hardness (112 HV) more than four passes of FSP (82 HV) but it is lower as compared to base alloy hardness (137 HV). It is clear from the **Fig. 7** that micro hardness decreases with the increasing number of pass. High hardness of the as-received base alloy is due to T651 treatment (solutionized, quenched, stress relieved and artificially aged) condition. The hardness reduction in the FSPed specimens can be attributed to the dissolution or over aging of the precipitates due to high temperature exposure. After FSP, microstructural softening (reduction in hardness) is common in precipitation hardened aluminum alloys and this softening can be reflected in deterioration of mechanical properties. In earlier studies also softening or low hardness of SZ of FSPed T6 condition aluminium alloy was reported **[24, 25]**.In a study of multi-layer friction deposition of AA2014-T6the inferior hardness was attributed to the over aged strengthening precipitates rather than the dissolution of precipitates **[26]**. However, in FSP of AA6061-T6, it was reported that microstructural softening or low hardness in SZ due to dissolution of the precipitates **[25]**. In another study it was indicated that softening of SZ in FSP of AA6082-T651 alloy due to the decomposition of hardening precipitates, over ageing of precipitates and low dislocation density **[24]**.

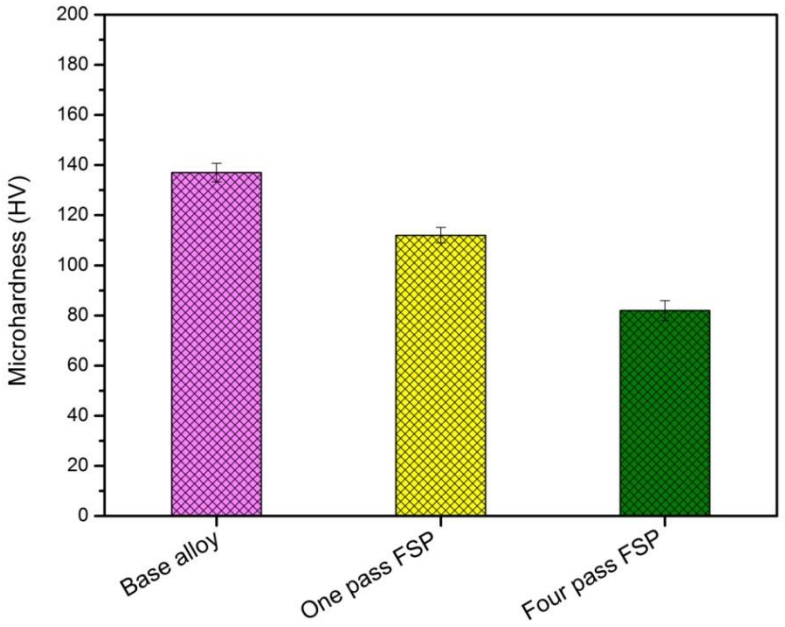

Fig. 7: Microhardness of base alloy, one pass and four pass FSPed specimens.

In four pass FSP specimen experienced four thermal cycles as that of only one cycle in one pass FSP. Therefore, hardening precipitates of four pass FSPed are over aged and resulted in reduction of hardness. Nonetheless, after four passes of FSP, significant grain refinement occurs but its contribution to hardness is limited as compared to the precipitates contribution. It is well known that the small precipitates distributed in the matrix contribute to the improvement in mechanical properties by hindering the moving dislocations. As size of the precipitates increases its effectiveness in restricting the dislocations decreases. On thermal exposure the small precipitates tend to agglomerate by diffusion mechanism and forms coarser precipitates. The schematic of overaging of the precipitates is shown in **Fig. 8**. It can be inferred that the hardness in a heat treated aluminum alloy is mainly governed by precipitates rather than the grain refinement.

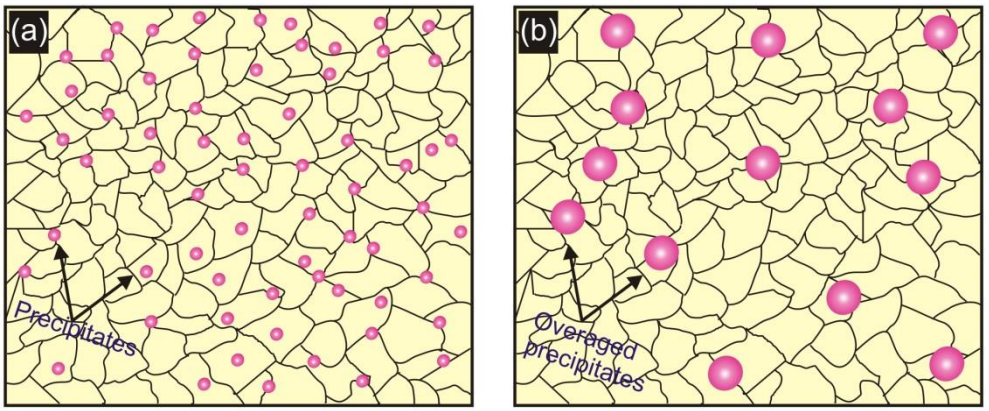

Fig. 8: Schematic of the coarsening of the fine precipitates.

3.3 Tensile strength:

Figure 9 shows the Stress-Strain curves for base alloy, one pass and four pass FSPed specimen. A reduction in tensile strength is observed for FSPed specimens in comparison to the base alloy specimen in spite

of the significant grain refinement. The base alloy shows maximum ultimate tensile strength (UTS) and UTS exhibits a decreasing trend from one pass to four pass FSP. The UTS is ~ 455 MPa for base alloy, while it is ~369 and ~278 MPa for the one pass and four passes FSPed specimens, respectively. Microstructural softening as discussed earlier in multi-pass FSP resulted in reduction of the UTS. One pass FSPed specimen exhibits decreased UTS as that of the base alloy but a two-fold increase in the ductility is observed. However, the ductility of the four pass of FSPed specimen is similar to the base alloy. Numerous studies reported higher UTS and increased elongation percentage for one pass FSPed specimen in comparison to multi-pass FSPed specimen **[27, 28]**.

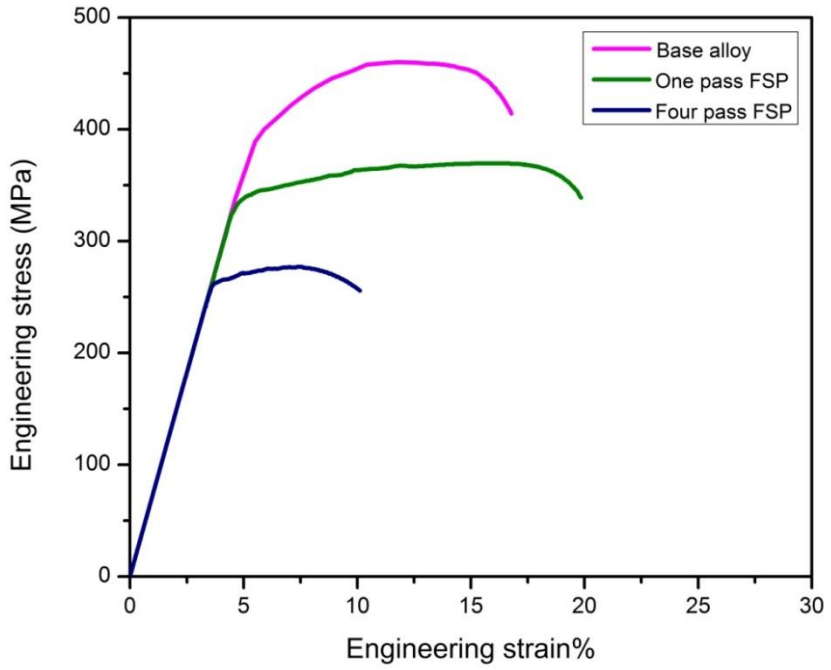

Fig. 9. Stress-strain curves for base alloy, one pass and four passFSP specimens.

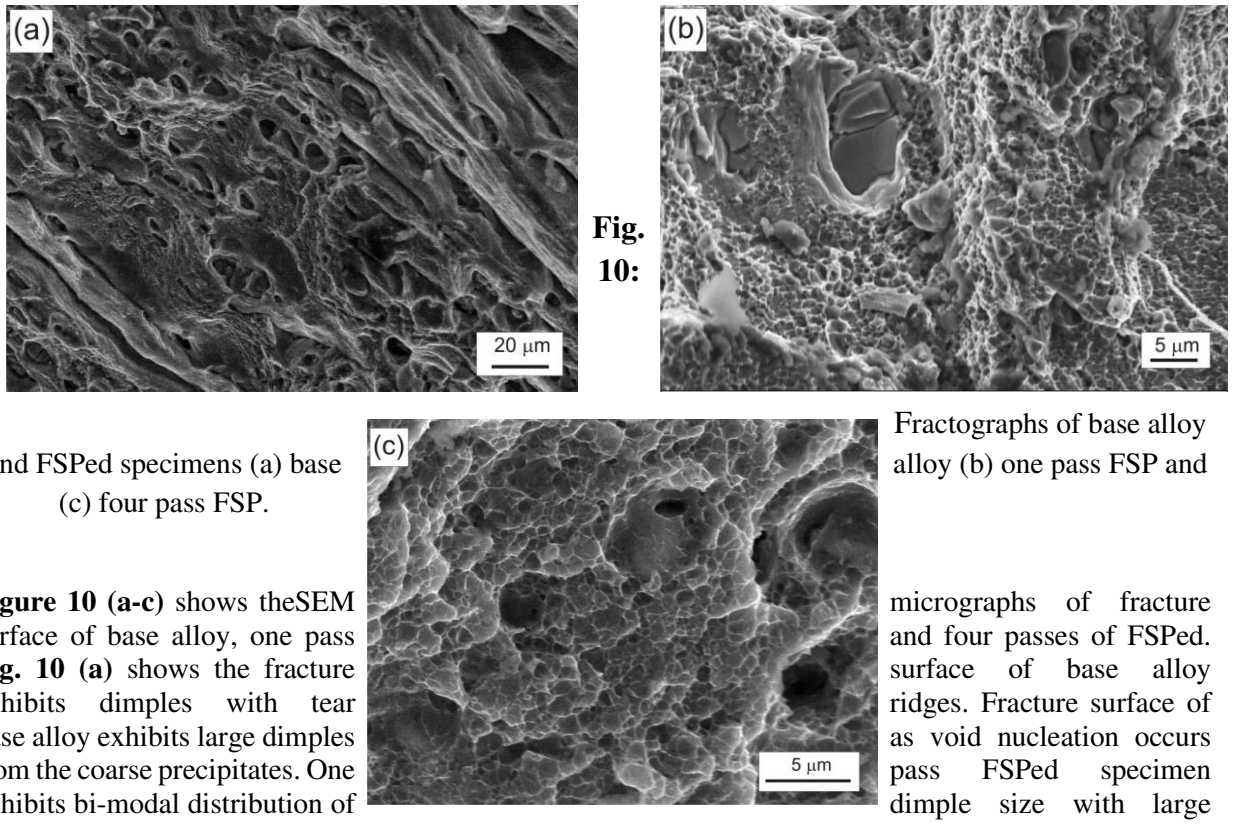

Fig. 10: Fractographs of base alloy and FSPed specimens (a) base alloy (b) one pass FSP and (c) four pass FSP.

Figure 10 (a-c) shows theSEM micrographs of fracture surface of base alloy, one pass and four passes of FSPed. **Fig. 10 (a)** shows the fracture surface of base alloy ridges. Fracture surface of exhibits dimples with tear as void nucleation occurs base alloy exhibits large dimples pass FSPed specimen from the coarse precipitates. One dimple size with large exhibits bi-modal distribution of dimples nucleating from coarse precipitates and small dimples originating from aluminum matrix **(Fig. 10b)**. Cracking of coarse precipitates is also observed in fracture surface of one pass FSPed specimen. In one pass FSPed specimen, a few coarse precipitates still exists as it is subjected to only one pass. Four passes of FSPed specimen fracture surface shows fine dimples with few large dimples **(Fig. 10c)**. Four pass FSP resulted in distribution and break up of coarse precipitates in the matrix. The fine and closely spaced dimples are originated from the fine precipitates. Some shallow dimples are also observed, suggesting the joining of micro-voids by shear deformation.

3.4 Fracture toughness

Fracture toughness of the one and four pass of FSP is decreased as compared to the fracture toughness of the base alloy as shown in **Fig. 11**. The base alloy's fracture toughness (40. 86 $MPam^{1/2}$) is decreased to about half after one pass FSP (21.05 $MPam^{1/2}$). After four pass of FSP the fracture toughness decreased to 14.67 $MPam^{1/2}$.The hardening precipitates in the base alloy effectively restrict the crack propagation or bypass the crack, thus increasing the crack length. After FSP the hardening precipitates loses their strength and crack easily propagates. The grain refinement occurred during FSP is not pronounced in providing the fracture resistance to FSPed specimens. A similar trend of variation in experimental fracture toughness was observed for 2024 T-3 FSW joints **[29]**. Load versus crack opening displacement curves is obtained experimentally are shown in **Fig.12**. The Fig. 12 indicates that base alloy can bear maximum load in comparison to the FSPed alloy.

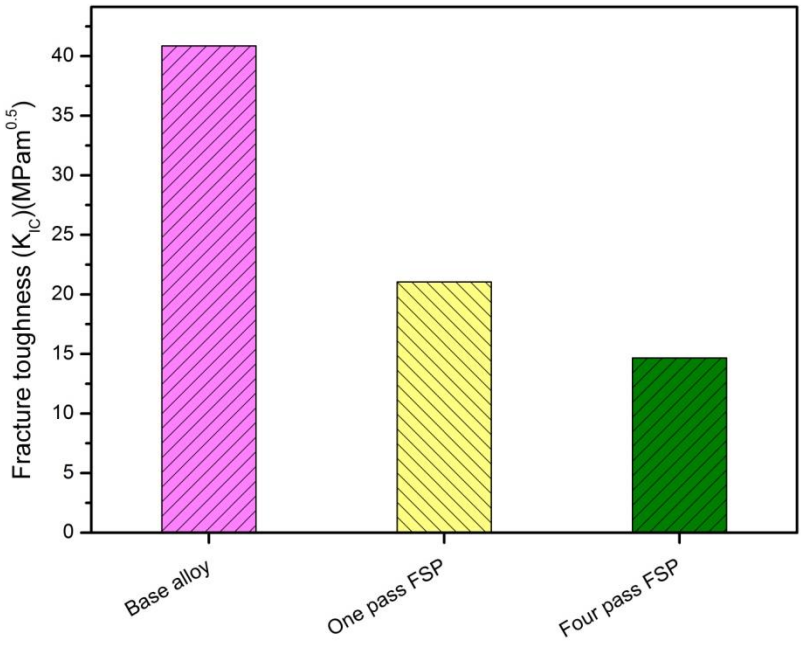

Fig. 11: Fracture toughness of the base alloy, one pass FSP and four pass FSP

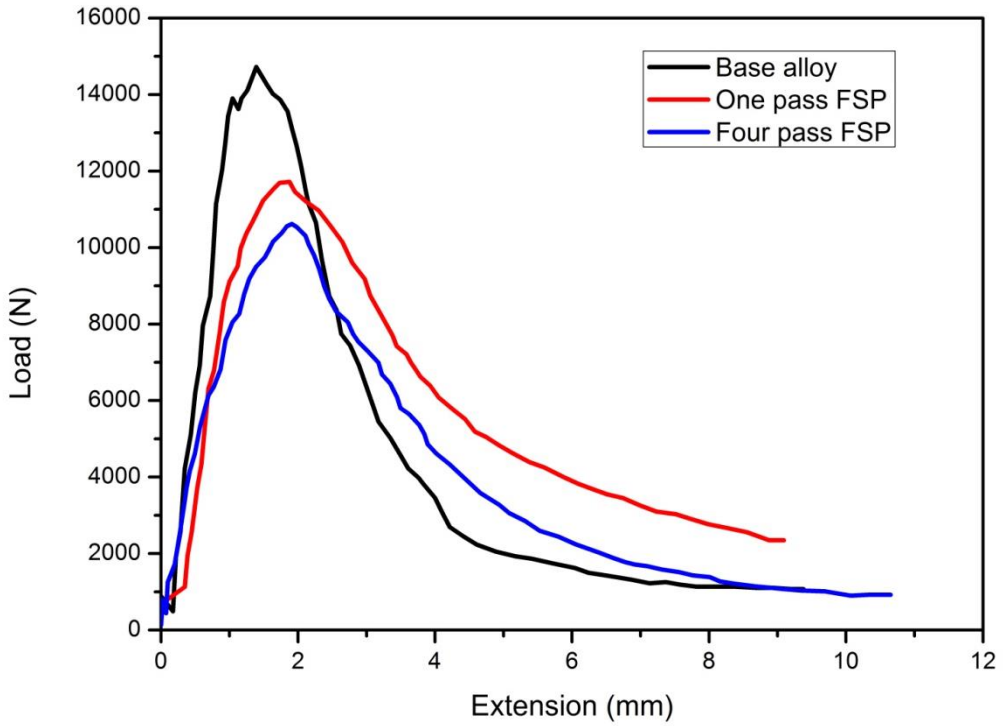

Fig. 12: Load versus extension curve of base alloy and FSPed specimen.

4. Conclusions:

In this study aluminum alloy AA2014-T651 is multi-pass FSPed with one and four pass at a constant rotational speed and traverse speed of 1000 rpm and 63 mm/min, respectively. The multiple pass FSP was performed with 100% overlapping. The following are the major conclusion drawn from the present study:
1. In multi-pass FSP the SZ area increases due to repetitive deformation and more number of thermal cycles. The SAZ also merges with SZ to contribute in the increase of SZ area.
2. FSP resulted in a significant grain refinement from average size of 125µm to 7µm after four pass. After one pass of FSP grain size decreased to 12µm which is about 10 times reduction in grain size as compared to the base alloy. However, after one pass FSP the grain size reduction is limited.
3. Microhardness of the FSPed alloy exhibited a decreasing trend on increasing the number of FSP pass. The repetitive thermal cycles causes overaging of the hardening precipitates which resulted in decrease in the micro hardness on increasing the FSP pass. Hardness contribution of grain refinement is limited as compared to the hardness contribution from the precipitates.
4. Tensile strength of the one pass FSPed alloy exhibited decrease in strength but showed improved ductility as compared to the base alloy. Nonetheless, after four pass of FSP both strength and ductility were decreased.
5. Fracture surface of base alloy and FSPed alloy showed dimples suggesting the ductile fracture. The fracture mechanism was governed by the size of the precipitates.
6. Similar to microhardness and tensile strength the fracture toughness also exhibits the decreasing trend with the increase in the passes of FSP. The base alloy shows maximum fracture toughness due to strengthening precipitates which easily restrict or bypass the crack propagation.

References :

[1] Mirzadeh, H. (2023). Surface metal-matrix composites based on AZ91 magnesium alloy via friction stir processing: A review. International Journal of Minerals, Metallurgy and Materials, 30(7), 1278-1296.
[2] Mishra RS, Ma ZY, Charit I (2003) Friction stir processing: a novel technique for fabrication of surface composite, Mat Sci Eng A 341:307-310.
[3] Sharma, C., Dwivedi, D. K., Kumar, P. (2013). Heterogeneity of microstructure and mechanical properties of friction stir welded joints of Al-Zn-Mg alloy AA7039. Procedia Engineering, 64, 1384-1394.
[4] Aliabadi, M., Khodabakhshi, F., Soltani, R., & Gerlich, A. P. (2023). Modification of flame-sprayed NiCrBSi alloy wear-resistant coating by friction stir processing and furnace re-melting treatments. Surface and Coatings Technology, 455, 129236.
[5] Li, Y., Guan, Y., Liu, Y., Zhai, J., Hu, K., & Lin, J. (2023). Microstructure and tensile properties of the friction stir processed LA103Z alloy. Materials Characterization, 196, 112616.
[6] Singh Yadav, R. K., Sharma, V., & Venkata Manoj Kumar, B. (2019). On the role of sliding load and heat input conditions in friction stir processing on tribology of aluminium alloy–alumina surface composites. Tribology-Materials, Surfaces & Interfaces, 13(2), 88-101.
[7] Sharma, V., & Tripathi, P. K. (2022). Approaches to measure volume fraction of surface composites fabricated by friction stir processing: a review. Measurement, 193, 110941.
[8] Yang, Y., Paidar, M., Mehrez, S., Ojo, O. O. (2022). Enhancement of mechanical properties and wear of AA5083/316 stainless steel surface-composite developed through multi-pass friction stir processing (MPFSP). Archives of Civil and Mechanical Engineering, 23(1), 13.
[9] Elyasi, M., Razaghian, A., Moharami, A., Emamy, M. (2022). Effect of Zirconium micro-addition and multi-pass friction stir processing on microstructure and tensile properties of Mg–Zn–Si alloys. Journal of Materials Research and Technology, 20, 4269-4282.
[10] Zhang, L., Liu, C. Y., Zhang, B., Huang, H. F., Xie, H. Y., & Cao, K. (2023). Mechanical properties of Al–Mg alloys with equiaxed grain structure produced by friction stir processing. Materials Chemistry and Physics, 294, 127010.

[11] Faraji, G., Dastani, O., & Mousavi, S. A. A. A. (2011). Effect of process parameters on microstructure and micro-hardness of AZ91/Al2O3 surface composite produced by FSP. Journal of Materials Engineering and Performance, 20, 1583-1590.
[12] Sharma, V., Kumar, P. S., & Pandey, O. P. (2012). Correlation of reinforced ceramic particle's nature and size with microstructure and wear behavior of Al-Si alloy composite. Advanced Materials Research, 585, 564-568.
[13]Singla, Y. K., Chhibber, R., Avdesh, Goyal, S., & Sharma, V. (2018). Influence of single and dual particle reinforcements on the corrosion behavior of aluminum alloy based composites. Proceedings of the Institution of Mechanical Engineers, Part L: Journal of Materials: Design and Applications, 232(6), 520-532.
[14] Eivani, A. R., Mehdizade, M., Chabok, S., & Zhou, J. (2021). Applying multi-pass friction stir processing to refine the microstructure and enhance the strength, ductility and corrosion resistance of WE43 magnesium alloy. journal of materials research and technology, 12, 1946-1957.
[15] Cui, G. R., Ni, D. R., Ma, Z. Y., & Li, S. X. (2014). Effects of friction stir processing parameters and in situ passes on microstructure and tensile properties of Al-Si-Mg casting. Metallurgical and Materials Transactions A, 45, 5318-5331.
[16] Venkateswarlu, G., Devaraju, D., Davidson, M. J., Kotiveerachari, B., & Tagore, G. R. N. (2013). Effect of overlapping ratio on mechanical properties and formability of friction stir processed Mg AZ31B alloy. Materials & Design, 45, 480-486.
[17] Gandra, J., Miranda, R. M., & Vilaça, P. (2011). Effect of overlapping direction in multipass friction stir processing. Materials Science and Engineering: A, 528(16-17), 5592-5599.
[18] Jana, S., Mishra, R. S., Baumann, J. A., & Grant, G. (2010). Effect of process parameters on abnormal grain growth during friction stir processing of a cast Al alloy. Materials Science and Engineering: A, 528(1), 189-199.
[19] Hu, K., Guan, Y., Zhai, J., Li, Y., Chen, F., Liu, Y., & Lin, J. (2022). Effect on microstructure and properties of LA103Z Mg–Li alloy plate by multi-pass friction stir processing. Journal of Materials Research and Technology, 20, 3985-3994.
[20] Mehdi, H., & Mishra, R. S. (2023). Modification of microstructure and mechanical properties of AA6082/ZrB2 processed by multipass friction stir processing. Journal of Materials Engineering and Performance, 32(1), 285-295.
[21] McNelley, T. R., Swaminathan, S., & Su, J. Q. (2008). Recrystallization mechanisms during friction stir welding/processing of aluminum alloys. Scripta materialia, 58(5), 349-354.
[22] Sharma, V., Kumar, S., Dewang, Y., & Nagpal, P. K. (2022). Post-processing of stir casted Al–Si12Cu metal matrix composite by friction stir processing. International Journal of Metalcasting, 16(4), 1985-1994.
[23] Bauri, R., Yadav, D., & Suhas, G. (2011). Effect of friction stir processing (FSP) on microstructure and properties of Al–TiC in situ composite. Materials Science and Engineering: A, 528(13-14), 4732-4739.
[24] Magdy M. El-Rayes, and Ehab A. El-Danaf, 'The influence of multi-pass friction stir processing on the microstructural and mechanical properties of aluminum alloy 6082', Journal of Materials Processing Technology, 212 (2012), 1157-1168.
[25] Wanchuck Woo, Hahn Choo, Donald W. Brown, and Zhili Feng, 'Influence of the tool pin and shoulder on microstructure and natural aging kinetics in a friction-stir-processed 6061-T6 Aluminum Alloy', Metallurgical and Materials Transactions A, 38 (2007), 69-76.
[26] Dilip, J. J. S., & Ram, G. J. (2013). Microstructure evolution in aluminum alloy AA 2014 during multi-layer friction deposition. Materials characterization, 86, 146-151.
[27] A. Alavi Nia, H. Omidvar, and S. H. Nourbakhsh, 'Effects of an Overlapping Multi-Pass Friction Stir Process and Rapid Cooling on the Mechanical Properties and Microstructure of AZ31 Magnesium Alloy', Materials & Design, 58 (2014), 298-304.

[28] Khaled J. Al-Fadhalah, Abdulla I. Almazrouee, and Abdulkareem S. Aloraier, 'Microstructure and Mechanical Properties of Multi-Pass Friction Stir Processed Aluminum Alloy 6063', Materials & Design, 53 (2014), 550-60.
[29] Sutton, M. A., Reynolds, A. P., Yang, B., & Taylor, R. (2003). Mixed mode I/II fracture of 2024-T3 friction stir welds. Engineering Fracture Mechanics, 70(15), 2215-2234.